

---

# Bayesian generative models can flag performance loss and bias

---

Anonymous Author(s)

Affiliation  
Address  
email

## Abstract

1 Generative models are popular for medical imaging tasks such as anomaly detection,  
2 feature extraction, data visualization, or image generation. Since they are  
3 parameterized by deep learning models, they are often sensitive to distribution  
4 shifts and unreliable when applied to out-of-distribution data, creating a risk of,  
5 e.g. underrepresentation bias. This behavior can be flagged using uncertainty  
6 quantification methods for generative models, but their availability remains limited.  
7 We propose SLUG: A new UQ method for VAEs that combines recent advances in  
8 Laplace approximations with stochastic trace estimators to scale gracefully with  
9 image dimensionality. We show that our UQ score – unlike the VAE’s encoder vari-  
10 ances – correlates strongly with reconstruction error and racial underrepresentation  
11 bias for dermatological images.

12 

## 1 Introduction

13 Variational Autoencoders (VAEs) stand out as one of the most widely used generative models in  
14 medical imaging because of their capacity to learn semantic, low-dimensional latent spaces. VAEs

15 are often used to analyze and manipulate key characteristics of high-dimensional data, e.g. for data

16 visualization [3], data generation [8], and anomaly detection [14].

17 Despite these advantages, generative models are parameterized with modern Deep Neural Networks  
18 (DNNs), which struggle with out-of-distribution (OOD) [13]. To tackle OOD performance in  
19 predictive models, uncertainty quantification (UQ) has emerged as an important tool [9], where the  
20 prediction is endowed with an associated uncertainty. This has proven useful for detecting silent  
21 failures and ensuring that unexpected outcomes do not occur. While UQ techniques have been  
22 proposed and studied with promising success for discriminative models [1], their applicability to  
23 generative models such as VAEs is underexplored. The adoption of a Bayesian approach can help  
24 address this issue; however, current Bayesian generative models tend to be computationally expensive,  
25 difficult to tune, or rely on uncorrelated posterior approximations [12, 2].

26 **We propose** a novel epistemic UQ method for VAEs building on the *Sketched Lanczos Uncertainty*  
27 (*SLU*) algorithm recently proposed for discriminative models [11]. SLU computes a rank- $k$  approxi-  
28 mation of the *generalized Gauss-Newton (GNN)* matrix, which captures the epistemic uncertainty  
29 according to a Laplace approximation [7]. However, SLU scales quadratically with the output dimen-  
30 sion, which is intractable in image-generative models. Our proposed *Sketched Lanczos Uncertainty*  
31 (*Global (SLUG)*) measure overcomes this challenge using scalable stochastic trace estimators [6] to  
32 produce a per-image score.

33 **We demonstrate SLUG’s ability** to detect underrepresentation bias in dermatological images. It is  
34 well known that dark skin tones are severely underrepresented in public datasets and that DNNs-based

35 systems tend to reproduce and amplify this bias [5, 10]. Our experiments show that SLUG strongly  
36 correlates with the performance of the VAE and can serve to flag both bias and performance loss.

37 In short, **we contribute** a novel UQ method for VAEs that capture out-of-distribution data and  
38 demonstrate its utility in flagging errors and underrepresentation bias using two publicly available  
39 real-world dermatology datasets: Fitzpatrick17k [5], and PASSION [4].

## 40 2 Method

41 Given the VAE  $f_{\phi, \theta}$  with encoder and decoder parameters  $(\phi, \theta) \in \mathbb{R}^p$ , we define its Jacobian  
42  $\mathbf{J}_{\{\phi, \theta\}}$  with respect to parameters and construct the Generalized Gauss-Newton (GGN) matrix as  
43  $\mathbf{G}_{\{\phi, \theta\}} = \sum_{i=1}^n \mathbf{J}_{\{\phi, \theta\}}(x_i)^T \mathbf{H}(x_i) \mathbf{J}_{\{\phi, \theta\}}(x_i)$ , where  $\mathbf{H}(x_i)$  is the Hessian of the loss w.r.t. to the  
44 neural network output and  $\{x_i \in \mathbb{R}^{W \times H \times C}\}_{i=1}^n$  the training set.

45 The GGN commonly appears as the inverse covariance of the *linearized Laplace approximation (LLA)*  
46 to the true posterior [7]. Currently, LLA is the most promising Bayesian posterior approximation [7],  
47 but it is, unfortunately, intractable for generative models as its computational cost scales quadratically  
48 with the generated data dimension, specifically  $\mathcal{O}((WHC)^2 p)$  for a network with  $p$  parameters.

49 Recently, Miani et al. [11] developed a sketching-based algorithm to evaluate the associated predictive  
50 uncertainty, which scales logarithmically with  $p$ . The resulting *Sketched Lanczos Uncertainty (SLU)*  
51 algorithm, however, still scales quadratically with the image dimension, making it impractical for  
52 VAEs. Our approach extends SLU to scale gracefully to large images.

### 53 2.1 Scaling to VAEs: Sketched Lanczos Uncertainty Global score (SLUG)

54 We based our proposed score on the SLU algorithm [11]. Let  $\mathbf{U}$  denote the matrix containing the  
55 leading eigenvectors of the GGN, then the SLU approximates the predictive variance of the linearized  
56 Laplace approximation with  $\mathbf{I} - \mathbf{U}\mathbf{U}^\top$  is covariance, i.e., for a specific pixel  $(w, h, c)$ ,

$$\text{SLU}_{w,h,c}(x) = e_{whc} \mathbf{J}_{\theta^*}(x) (\mathbf{I} - \mathbf{U}\mathbf{U}^\top) \mathbf{J}_{\theta^*}(x)^\top e_{whc}^\top, \quad (1)$$

57 where  $e_{whc}$  is a one-hot encoding vector that selects the pixel position to compute the uncertainty.

58 SLU approximates this predictive uncertainty using several tricks from randomized numerical linear  
59 algebra. Unfortunately, even SLU does not scale to neural networks with high-dimensional outputs  
60 like those in generative models. Producing one predictive variance per generated pixel requires  
61  $\mathcal{O}(WHC)$  SLU invocations, which is practically prohibitive. Our main interest is in measuring  
62 a scalar uncertainty score for a generated image, and we choose the sum of per-pixel predictive  
63 variances, which we denote the *Sketched Lanczos Uncertainty Global (SLUG)* score. We use a  
64 stochastic trace estimator [6] to estimate the SLUG score,

$$\text{SLUG}(x) = \sum_{w,h,c} \text{SLU}_{w,h,c}(x) \quad (2)$$

$$= \text{Tr}(\mathbf{J}_{\theta^*}(x) (\mathbf{I} - \mathbf{U}\mathbf{U}^\top) \mathbf{J}_{\theta^*}(x)^\top) \quad (3)$$

$$\approx \frac{1}{S} \sum_{s=1}^S \epsilon_s \mathbf{J}_{\theta^*}(x) (\mathbf{I} - \mathbf{U}\mathbf{U}^\top) \mathbf{J}_{\theta^*}(x)^\top \epsilon_s^\top, \quad (4)$$

65 where  $\epsilon_s \sim \mathcal{N}(0, \mathbf{I})$ . This can be implemented using only  $S$  invocations of SLU.

## 66 3 Experiments and results

67 **Datasets.** In our experiments, we use two dermatology datasets. The VAE is trained on the  
68 **Fitzpatrick17k** dataset [5], which includes 16,577 images labeled with Fitzpatrick skin types (FST).  
69 To evaluate the impact of skin tone representation in the training data, we create three subsets of  
70 1,668 images each: **Dataset A – Light** (100% FST 1–2), **Dataset B – Mixed** (50% FST 1–2 and 50%  
71 FST 5–6), and **Dataset C – Black** (100% FST 5–6). Two separate test sets of 512 images each are  
72 sampled for lighter and darker skin tones. For external validation and to assess model bias, we use  
73 the **PASSION** dataset [4], which contains 4,901 dermatology images from Sub-Saharan countries  
74 with darker skin tones (FST 3–6).

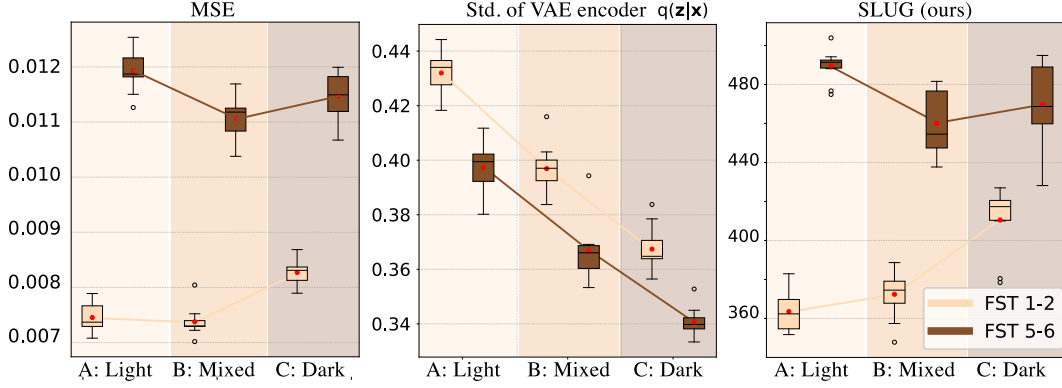


Figure 1: On Fitzpatrick17k, the performance on light and dark skin tones changes with their representation. The VAE encoder uncertainty is a poor indicator, while SLUG follows performance across groups and training scenarios.

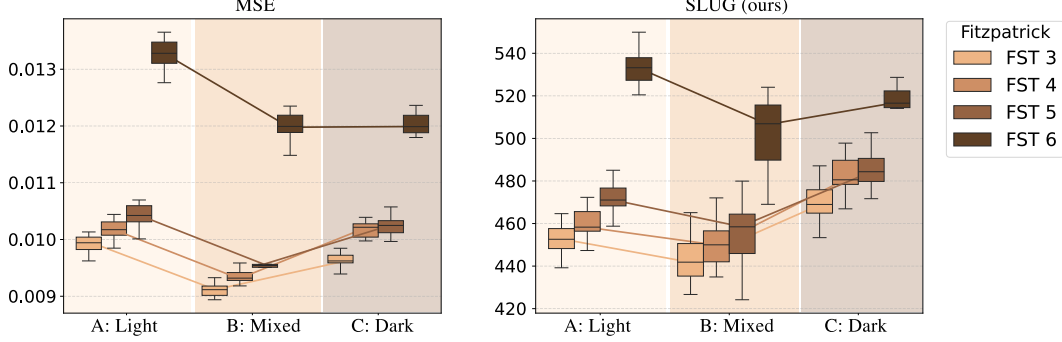


Figure 2: On the external PASSION dataset, we see again how reduced MSE is flagged by increased SLUG uncertainty across dark skin tone groups.

75 **Racial bias.** Fig. 1 shows that SLUG effectively captures racial bias in the Fitzpatrick17k  
76 dataset—unlike the VAE’s latent uncertainty. We also evaluate the trained models in Fitzpatrick17k  
77 on the external PASSION dataset. The results reveal a consistent pattern: performance degrades as  
78 skin tone darkens (see Fig. 2). Notably, our SLUG score also captures this racial bias in the external  
79 dataset, highlighting its utility as a metric to flag bias.

## 80 4 Conclusion

81 This work highlights the urgent need for precise and scalable UQ for generative models. Despite the  
82 widespread use of generative AI, we still lack a reliable mechanism to ensure its trustworthiness. **We**  
83 **demonstrate that epistemic UQ can warn of performance loss, and detect bias.**

84 We expect that these results will motivate the recognition of epistemic uncertainty as an essential tool  
85 for generative models. While our SLUG method for VAEs can capture bias and performance loss in  
86 dermatological images, it will be valuable to see how epistemic uncertainty and bias interact in other  
87 large generative models, such as diffusion models.

## 88 5 Potential Negative Impact Statement

89 This paper studies the relationship between epistemic uncertainty and racial bias in dermatology  
90 using generative models, evaluated on the Fitzpatrick17k and a Sub-Saharan dataset. The analysis is  
91 limited to racial categories present in these datasets and does not consider other sources of bias, such  
92 as gender, age, or data origin. These unexamined factors may also influence uncertainty and model  
93 performance.

94 The models are evaluated on curated datasets and not tested under out-of-distribution or real-world  
95 clinical conditions. As a result, their robustness and reliability in practice remain unclear. Further  
96 evaluation in real-world and OOD settings is necessary to assess clinical safety.

97 While the method proposed may help identify racial bias, they do not prevent misuse or biased  
98 deployment. Ensuring fairness in clinical applications requires broader efforts, including careful  
99 validation, and responsible use by practitioners and developers.

## 100 References

- 101 [1] Moloud Abdar, Farhad Pourpanah, Sadiq Hussain, Dana Rezazadegan, Li Liu, Mohammad  
102 Ghavamzadeh, Paul Fieguth, Xiaochun Cao, Abbas Khosravi, U Rajendra Acharya, et al. “A  
103 review of uncertainty quantification in deep learning: Techniques, applications and challenges”.  
104 In: *Information fusion* 76 (2021), pp. 243–297.
- 105 [2] Erik Daxberger and José Miguel Hernández-Lobato. “Bayesian variational autoencoders for  
106 unsupervised out-of-distribution detection”. In: *arXiv preprint arXiv:1912.05651* (2019).
- 107 [3] Jan Ehrhardt and Matthias Wilms. “Autoencoders and variational autoencoders in medical  
108 image analysis”. In: *Biomedical Image Synthesis and Simulation*. Elsevier, 2022, pp. 129–162.
- 109 [4] Philippe Gottfrois, Fabian Gröger, Faly Herizo Andriambololaina, Ludovic Amruthalingam,  
110 Alvaro Gonzalez-Jimenez, Christophe Hsu, Agnes Kessy, Simone Lionetti, Daudi Mavura,  
111 Wingston Ng’ambi, et al. “PASSION for Dermatology: Bridging the Diversity Gap with  
112 Pigmented Skin Images from Sub-Saharan Africa”. In: *International Conference on Medical  
113 Image Computing and Computer-Assisted Intervention*. Springer. 2024, pp. 703–712.
- 114 [5] Matthew Groh, Caleb Harris, Luis Soenksen, Felix Lau, Rachel Han, Aerin Kim, Arash  
115 Koochek, and Omar Badri. “Evaluating deep neural networks trained on clinical images in  
116 dermatology with the Fitzpatrick 17k dataset”. In: *Proceedings of the IEEE/CVF Conference  
117 on Computer Vision and Pattern Recognition*. 2021, pp. 1820–1828.
- 118 [6] Michael F Hutchinson. “A stochastic estimator of the trace of the influence matrix for Laplacian  
119 smoothing splines”. In: *Communications in Statistics-Simulation and Computation* 18.3 (1989),  
120 pp. 1059–1076.
- 121 [7] Alexander Immer, Maciej Korzepa, and Matthias Bauer. “Improving predictions of Bayesian  
122 neural nets via local linearization”. In: *International conference on artificial intelligence and  
123 statistics*. PMLR. 2021, pp. 703–711.
- 124 [8] Lennart R Koetzier, Jie Wu, Domenico Mastrodicasa, Aline Lutz, Matthew Chung, W Adam  
125 Koszek, Jayanth Pratap, Akshay S Chaudhari, Pranav Rajpurkar, Matthew P Lungren, et al.  
126 “Generating synthetic data for medical imaging”. In: *Radiology* 312.3 (2024), e232471.
- 127 [9] Benjamin Kompa, Jasper Snoek, and Andrew L Beam. “Second opinion needed: communicating  
128 uncertainty in medical machine learning”. In: *NPJ Digital Medicine* 4.1 (2021),  
129 p. 4.
- 130 [10] Miguel López-Pérez, Søren Hauberg, and Aasa Feragen. “Are generative models fair? a study  
131 of racial bias in dermatological image generation”. In: *Scandinavian Conference on Image  
132 Analysis*. Springer. 2025, pp. 389–402.
- 133 [11] Marco Miani, Lorenzo Beretta, and Søren Hauberg. “Sketched Lanczos uncertainty score:  
134 a low-memory summary of the Fisher information”. In: *Advances in Neural Information  
135 Processing Systems*. Ed. by A. Globerson, L. Mackey, D. Belgrave, A. Fan, U. Paquet, J.  
136 Tomczak, and C. Zhang. Vol. 37. 2024, pp. 23123–23154.
- 137 [12] Marco Miani, Frederik Warburg, Pablo Moreno-Muñoz, Nicki Skafte, and Søren Hauberg.  
138 “Laplacian autoencoders for learning stochastic representations”. In: *Advances in Neural  
139 Information Processing Systems* 35 (2022), pp. 21059–21072.
- 140 [13] Anh Nguyen, Jason Yosinski, and Jeff Clune. “Deep neural networks are easily fooled: High  
141 confidence predictions for unrecognizable images”. In: *Proceedings of the IEEE conference  
142 on computer vision and pattern recognition*. 2015, pp. 427–436.
- 143 [14] Hansen Wijanarko, Evelyne Calista, Li-Fen Chen, and Yong-Sheng Chen. “Tri-VAE: Triplet  
144 Variational Autoencoder for Unsupervised Anomaly Detection in Brain Tumor MRI”. In:  
145 *Proceedings of the IEEE/CVF Conference on Computer Vision and Pattern Recognition*. 2024,  
146 pp. 3930–3939.